Small-molecule PKR-like endoplasmic reticulum kinase inhibitors as a novel targeted therapy for Parkinson's disease

WERONIKA LUSA[1], WIOLETTA ROZPĘDEK-KAMIŃSKA[1], NATALIA SIWECKA[1], GRZEGORZ GALITA[1], IRENEUSZ MAJSTEREK[1] and EWA KUCHARSKA[2]

[1]Department of Clinical Chemistry and Biochemistry, Medical University of Lodz, 92-213 Lodz; [2]Department of Geriatrics and Social Work, Jesuit University Ignatianum in Krakow, 31-501 Krakow, Poland

Received October 20, 2022; Accepted January 23, 2023

DOI: 10.3892/mmr.2023.12989

Abstract. Parkinson's disease (PD) is the second most common neurodegenerative disorder in worldwide and remains a therapeutic challenge due to the low efficacy of current treatments. Numerous studies have demonstrated the pivotal role of endoplasmic reticulum (ER) stress in PD pathogenesis. ER stress, followed by activation of the protein kinase RNA-like endoplasmic reticulum kinase (PERK)-dependent branch of the unfolded protein response signaling pathway, ultimately leads to neural cell death and dopaminergic neurodegeneration in PD. Therefore, the present study evaluated the effectiveness of the small-molecule PERK inhibitor LDN-87357 in an *in vitro* PD model using the human neuroblastoma SH-SY5Y cell line. To assess the mRNA expression levels of the pro-apoptotic ER stress markers, the TaqMan Gene Expression Assay was performed. Cytotoxicity was assessed using a colorimetric 2,3-bis-(2-methoxy-4-nitro-5-sulfophenyl)-2H-tetrazolium-5-carboxanilide assay and apoptosis was assessed using a caspase-3 assay. Moreover, cell cycle progression was evaluated using flow cytometry. The results indicated that LDN-87357 treatment induced a significant decrease in ER stress markers gene expression in SH-SY5Y cells exposed to ER stress. Furthermore, LDN-87357 significantly increased viability, diminished apoptosis and restored the normal cell cycle distribution of SH-SY5Y cells after ER stress induction. Therefore, the evaluation of small-molecule PERK inhibitors, such as LDN-87357, may lead to the development of novel therapeutic strategies against PD.

Correspondence to: Professor Ireneusz Majsterek, Department of Clinical Chemistry and Biochemistry, Medical University of Lodz, Mazowiecka 5, 92-213 Lodz, Poland
E-mail: ireneusz.majsterek@umed.lodz.pl

Key words: Parkinson's disease, Parkinson's disease treatment, neurodegeneration, protein kinase RNA-like endoplasmic reticulum kinase, small-molecule PERK inhibitor, unfolded protein response, endoplasmic reticulum stress, apoptosis

Introduction

Parkinson's disease (PD) is a multifactorial neurodegenerative disease (1). It is the second most frequently diagnosed type of neurodegenerative disease (2) and its incidence ranges from 5/100,000 to over 35/100,000 new cases each year, according to worldwide data, mainly obtained from Europe and the USA (3), with this value significantly increasing from the sixth to ninth decade of life (4). The prevalence has grown with the aging population (4), and the number of individuals suffering from PD worldwide is projected to exceed 12 million by 2040 (5).

The main brain area affected by neurodegeneration in PD is the substantia nigra pars compacta (SNpc) in the midbrain, which demonstrates selective loss of dopaminergic neurons. However, during PD development, extensive involvement of other structures in either the central (e.g. in the basal ganglia, cerebellum or thalamus) (6) or peripheral (e.g. in the sensory nerves) (7) nervous system can be observed (8).

The clinical manifestation of PD is primarily based on motor symptoms like bradykinesia, muscle rigidity, resting tremor, posture and gait abnormalities (9). As the disease progresses, more advanced signs of neurodegeneration such as dysarthria and dysphagia can also occur (9). Furthermore, PD is associated with numerous non-motor symptoms, including hyposmia, sleep disturbances, bowel and urinary dysfunction and depression (10). One important clinical characteristic of PD is continuous cognitive decline, which increases with the progression of neurodegenerative processes (11).

In terms of PD development, several groups of risk factors can be distinguished. The first group comprises numerous genetic causes that have been identified in recent years. In most populations, 3-5% of PD cases could be explained by monogenic mutations (12) in genes such as synuclein α (*SNCA*; encoding α-synuclein), *VPS35* (involved in endosomal trafficking), parkinsonism associated deglycase and PTEN induced kinase 1 (mitochondrial genes), leucine rich repeat kinase 2 (serving a role in autophagy and microtubule stability) and *GBA* (encoding a key enzyme for the proper functioning of lysosomes) (13). In contrast, the hereditary risk of developing non-monogenic PD varies from 16-36% and at least 90 genetic risk variants have been reported overall (12). Sporadic/idiopathic PD is strongly age-related (14) and associated with a

heterogenous group of environmental risk factors including pesticides, low-frequency magnetic fields (15) or previous head injury (16).

The development of neurodegeneration at the cellular level has frequently been attributed to the accumulation of misfolded proteins; more specifically, the underlying central pathogenetic mechanism of PD is associated with the aggregation of misfolded α-synuclein (αS) protein. Following this, αS fibrils further accumulate to eventually form proteinaceous intracellular inclusion bodies in neuronal somas or neurites, called Lewy bodies or Lewy neurites, respectively (17). Furthermore, αS aggregates interact with the substrates of the outer mitochondrial membrane, which initiates mitochondrial dysfunction; this phenomenon occurs in both genetic and sporadic PD (18), and results in increased production of reactive oxygen species (ROS), which generate oxidative stress conditions and thus potentiate the neurodegeneration process in dopaminergic neurons (19). Moreover, pathological αS activity can stem from the malfunction of degradation pathways like the autophagy-lysosome system, which are responsible for toxicity control and cell death prevention by timely removal of long-lived proteins and impaired organelles (20).

As a consequence of these events, the accumulation of αS aggregates and the disruption of protein clearance trigger endoplasmic reticulum (ER) stress conditions within neural cells (21). The ER is an important eukaryotic organelle, which serves a vital role in the protein quality control system. It is involved in protein folding and regulates intracellular calcium levels (22). ER-related proteostasis is maintained by numerous specific chaperones, such as glucose-regulated protein 78 (GRP78) (23). As the misfolded proteins accumulate in the ER lumen, proteostasis becomes disrupted, which induces ER stress conditions. Subsequently, the unfolded protein response (UPR) signaling pathway is activated as an adaptive mechanism (24). Initially, the UPR may involve neuroprotective mechanisms and alleviate protein overload in the ER, but in the case of persistent ER stress, the UPR executes pro-apoptotic cascades that aggravate neurodegeneration (21). The UPR is controlled by three specific transmembrane proteins in the ER, which act as stress sensors: Activating transcription factor (ATF6), inositol-requiring enzyme 1 (IRE1) and protein kinase RNA-like ER kinase (PERK) (25). Under evoked ER stress conditions, activated PERK undergoes oligomerization and autophosphorylation. The phosphorylated form of PERK (p-PERK) in turn phosphorylates the a subunit of eukaryotic initiation factor 2α (eIF2α), which is involved in the repression of global protein synthesis by inhibition of the 80S ribosome assembly. Despite this, the activating transcription factor 4 (ATF4) mRNA undergoes preferential translation as a result of eIF2α activation, due to the presence of open reading frames in its 5'-untranslated region (26,27). One of the roles of ATF4 is to induce the transcription of the CCAAT enhancer binding protein homologous protein (CHOP) (28), which strongly promotes apoptotic cell death in neural cells (29). CHOP is encoded by the DNA damage-inducible transcript 3 *(DDIT3)* gene (30). Apoptosis induced by CHOP overexpression is associated with activation and mitochondrial translocation of protein (31). It has been reported that CHOP regulates the expression of certain proteins from the Bcl-2 family, including pro-apoptotic proteins (such as Bcl-2-like protein 11, p53 upregulated modulator of apoptosis and phorbol-12-myristate-13-acetate-induced protein 1), and upregulates the expression of proteins, such as DNA damage-inducible 34 (GADD34), Tribbles-related protein 3 and endoplasmic reticulum oxidoreductin 1α (32).

Previous studies have reported that ER dysfunction, ER stress conditions and UPR activation are key events in the pathogenesis of PD. For instance, *post mortem* examination of the brain tissues of PD patients has revealed elevated levels of the p-PERK and p-eIF2α (33). Furthermore, in an *in vivo* model of PD, the overexpression of ATF4, a crucial member of the PERK-dependent signaling pathway, resulted in severe dopaminergic neurodegeneration in the substantia nigra region (34). Moreover, it has been reported that aggregates of misfolded aS interact directly with the GRP78 chaperone, which results in UPR activation (17,35). A previous study reported that the interaction between αS aggregates and ER calcium pump, sarco/endoplasmic reticulum Ca^{2+}-ATPase (SERCA) induces cell sensitization to ROS production and apoptosis (36). It is important to notice that certain genetic mutations directly connected with the familial type of PD are also linked to ER dysfunction and UPR activation (25).

Contemporary therapeutic strategies for PD still only treat the symptoms and are mainly based on pharmacotherapy and non-pharmacological supporting methods (such as surgery or physiotherapy). Current pharmacological treatment of PD is focused on increasing the level of the neurotransmitter dopamine in the brain (12). This can be achieved using drugs which act on several pharmacological targets associated with dopamine metabolism, such as the dopamine precursor Levodopa, passing through blood-brain barrier (BBB), or dopamine degradation inhibitors (e.g. monoamine oxidase B inhibitors or catechol-o-methyltransferase inhibitors) (37). To the best of our knowledge, there is currently no available and approved therapy that can slow or halt the progression of the disease, and hence, prevent or reverse the ongoing neurodegeneration process (38).

As evidence from previous studies indicates that the ER stress and the PERK-dependent branch of the UPR may be strongly associated with PD pathogenesis at the molecular level, the present study evaluated the efficacy of the small-molecule PERK inhibitor LDN-87357 in an *in vitro* model of PD. Recent results indicated that targeting the individual components of the UPR signaling branches may lead to the development of innovative, disease-modifying therapeutic options for PD (25).

Materials and methods

Identification of the small-molecule PERK inhibitor LDN-87357. The investigated small-molecule PERK inhibitor LDN-87357 was screened, characterized and provided for further analysis courtesy of the Department of Biochemistry and Molecular Biology, Hollings Cancer Center (Medical University of South Carolina, USA). The selection was performed according to the protocol described previously by Pytel *et al* (39). High-throughput assay screening (inhibitor selection) was performed using the Laboratory for Drug Discovery in Neurodegeneration (LDDN) compound library; the LDDN is part of the Department of Neurology at Brigham and Women's Hospital and the Harvard Medical School

(Boston, MA, USA) (40). The library consists of 150,000 compounds, of which 80,000 were selected for further analysis based on certain computational filters that have previously been described (39). The calculations of desirability filters, such as polar surface area or Lipinski's 'rule of five' were performed to select the compounds with an increased probability of good oral bioavailability and ability to cross the BBB.

Cell culture. All experiments were performed using an *in vitro* model of PD with a commercially available neuroblastoma SH-SY5Y cell line, purchased from the American Type Culture Collection (ATCC; cat. no. CRL-2266TM), which is derived from human neuroblastoma tissues and widely used in PD research (41). The culture was maintained according to the supplier's protocol, under standard conditions, which were 37˚C, 5% CO_2 and 95% humidity. The complete culture medium for SH-SY5Y cells was composed of: ATCC-formulated Eagle's Minimum Essential Medium (EMEM) (cat. no. 30-2003TM; ATCC) and F12 Medium (cat. no. 11765-054; Thermo Fisher Scientific, Inc.), mixed in a 1:1 ratio. The medium was supplemented with 10% fetal bovine serum (cat. no. 30-2020; ATCC) and 100 U/ml penicillin with 100 μg/ml streptomycin solution (cat. no. 15140-122; Gibco; Thermo Fisher Scientific, Inc.). Cell passage was performed every 3-4 days (when cells reached 90-95% confluence). The cells were dissociated using 0.25% trypsin and 0.53 mM EDTA solution.

Analysis of the mRNA expression levels of the pro-apoptotic ER stress-related genes. To assess the mRNA expression levels of specific pro-apoptotic ER stress-related genes, total RNA was isolated from SH-SY5Y cells using a PureLink RNA Mini Kit (Thermo Fisher Scientific Inc.). The RNA obtained was reverse transcribed into complementary (c)DNA using GoScript TM Reverse Transcriptase (Promega Corporation) at a final concentration of 100 ng. All steps were performed in accordance with the manufacturers' protocols. Following this, TaqMan Gene Expression Assays were performed for the analysis of the expression of pro-apoptotic, ER stress-related genes, including *DDIT3*, *BAX*, *ATF4*, *eIF2α*, *Bcl-2*, *GADD34*. *ACTB* was used as a reference gene (details of the assays used were presented in Table I). The mixture for the qPCR analysis (with a total volume of 10 μl), consisted of the following reagents: cDNA (1 μl), 5x HOT FIREPol® Probe quantitative (q)PCR Mix (2 μl; Solis BioDyne OÜ), primers (1 μl) and nuclease free water (6 μl). The thermocycling conditions for the qPCR analysis were as follows: enzyme activation (15 min at 95˚C), DNA denaturation (40 cycles of 10 sec at 95˚C) and annealing/extension (40 cycles of 60 sec at 60˚C), according to the manufacturer's protocol. Gene expression was determined by the $2^{-\Delta\Delta Cq}$ quantification method (42) using a Bio-Rad CFX96 (Bio-Rad Laboratories, Inc.) system.

Analysis of the cytotoxicity and pharmacological efficacy of the LDN-87357. The cytotoxicity of the investigated PERK inhibitor, LDN-87357, was evaluated using the colorimetric 2,3-bis-(2-methoxy-4-nitro-5-sulfophenyl)-2 H-tetrazolium-5-carboxanilide (XTT) assay (Thermo Fisher Scientific, Inc.). The assay assessed cell viability as a function of the cellular redox potential. Actively-respiring cells transform XTT into an orange-colored formazan product, both of which are soluble in water. All experiments were repeated three times, with similar results. Briefly, SH-SY5Y cells were cultured in 96-well plates ($5x10^3$ cells/well) for 24 h at 37˚C in 100 μl complete growth medium. Cells were then exposed at 37˚C to 100 μl of complete culture medium containing LDN-87357, at the following concentrations: 0.75, 3, 6, 12, 25, 50, 75 or 100 μM, or 50 mM or 0.1% DMSO (MilliporeSigma), which was the solvent used for LDN-87357. Cells untreated with the inhibitor and cultured in complete medium were used as a negative control, whereas cells treated with 100% DMSO served as the positive control.

The present study also evaluated the effectiveness of LDN-87357 after the induction of ER stress conditions in SH-SY5Y cells. The cells were seeded in 96-well plates ($5x10^3$ cells/well) and cultured for 24 h in 100 μl of complete culture medium. After incubation, the cells were exposed to 100 μl complete culture medium containing LDN-87357 at the aforementioned concentration range for 1 h, and then treated with 500 nM thapsigargin (Th) to invoke ER stress. Certain cells were treated only with 500 nM Th. Cells cultured in complete medium only were used as a negative control, and 100% DMSO-treated cells were used as a positive control. All samples were incubated for 16, 24 or 48 h, and then 25 μl XTT/PMS mixture was added to each well and incubated for 2 h at 37˚C in a 5% CO_2 incubator. The absorbance was quantified using a Synergy HT spectrophotometer (Agilent Technologies, Inc.) at 450 nm.

Assessment of apoptosis using a caspase-3 activity assay. The activity of caspase-3, one of the major pro-apoptotic proteins, was assessed using the Caspase-3 Assay Kit (Colorimetric) (Abcam). Activated caspase-3 cleaved the labeled DEVD-p-NA substrate, and levels of the obtained product, chromophore p-nitroaniline (p-NA), were assessed using a spectrophotometer. All tests were performed in triplicate with similar results. Briefly, SH-SY5Y cells were cultured in 6-well plates ($5x10^5$ cells/well) in a complete culture medium for 24 h at 37˚C. The cells were then incubated for another 24 h at 37˚C with LDN-87357 (0.75, 3, 6, 12, 25, 50 and 100 μM) or with the solvent, 0.1% DMSO (MilliporeSigma). One set of cells was exposed to 1 μM staurosporine (cat. no. S4400-1MG; MilliporeSigma) for 16 h at 37˚C as a positive control, and another set of cells were cultured for 24 h in complete culture medium alone as a negative control. To assess the effectiveness LDN-87357 in SH-SY5Y cells exposed to ER stress, the cells were transferred to 6-well plates ($5x10^5$ cells/well) and the culture was maintained in complete medium for 24 h at 37˚C. The cells were then exposed to complete culture medium including LDN-87357 at the aforementioned concentration range for 1 h at 37˚C, and then Th was added at 500 nM for 24 h at 37˚C. An additional group of cells was treated only with 500 nM Th (cat. no. 58-600-51MG; MilliporeSigma) for 24 h at 37˚C. The positive control consisted of SH-SY5Y cells treated with 1 μM staurosporine for 16 h at 37˚C and the negative control consisted of cells incubated for 24 h at 37˚C in complete growth medium alone. After removal of complete medium, the SH-SY5Y cells were rinsed with 1X Dulbecco's phosphate-buffered saline (DPBS; MilliporeSigma). The cells were then passaged with 0.25% trypsin and 0.53 mM EDTA solution (ATCC) for 5 min at 37˚C. The obtained cell

Table I. Assays used for assessment of mRNA expression levels, using the TaqMan gene expression assay.

Gene	Assay ID	Chromosome location
DDIT3	Hs01090850_m1	Chr.12: 57516588-57520517
BAX	Hs00180269_m1	Chr.19: 48954825-48961798
ATF4	Hs00909569_g1	Chr.22: 39519709-39522686
eIF2α	Hs00230684_m1	Chr.3: 150546678-150586016
Bcl-2	Hs00608023_m1	Chr.18: 63123346-63319778
GADD34	Hs00169585_m1	Chr.19: 48872392-48876062
ACTB	Hs99999903_m1	Chr.7: 5527148-5530601

Chromosome location were based on the Genome Reference Consortium Human Build 38. *DDIT3, DNA damage-inducible transcript 3*; *ATF4*, *activating transcription factor 4*; *GADD34*, *DNA damage-inducible 34; ACTB, β-actin*.

suspension was then centrifuged at 140 x g for 5 min at room temperature. After removal of the supernatant, the cell pellet was resuspended in complete culture medium), counted using a TC20 Automated Cell Counter (Bio-Rad Laboratories, Inc.), centrifuged at 140 x g for 5 min at room temperature, and the final pellet (~1x10^6 cells) was then resuspended in 50 μl of cold Cell Lysis Buffer (Abcam). The cell suspension was incubated for 10 min on ice, and then centrifuged at 10,000 x g for 1 min at room temperature. The supernatant was then transferred to fresh 2 ml tubes. Protein concentration was assessed using a standard Bradford assay, with BSA used as a protein standard; each assay used cell lysate containing 100 μg of protein. Following this, each sample was supplemented with 2X Reaction Buffer (Abcam)(including DTT at 10 mM) and DEVD-pNA (4 mM) substrate (Abcam) at a final concentration of 200 μM. The cells were incubated for two h at 37˚C, and the p-NA level was assessed spectrophotometrically at 405 nm using a Synergy HT spectrophotometer (Agilent Technologies, Inc.).

Analysis of cell cycle distribution and progression. Cell cycle distribution was determined by flow cytometry using propidium iodide (PI) staining. Due to the inability of PI to penetrate living cells, prior treatment with ethanol was required. The method provided assessment of the cell cycle based on the differences in fluorescence intensity and the increased fluorescence present in cells preparing for division due to increased DNA levels. The cell cycle was interpreted based on the following phases: sub G0/G1 (representation of apoptotic cell subpopulation), G0/G1 (regulation of the entry of the quiescent cell into the cycle), S (DNA replication) and G2/M (checkpoint responsible for the prevention of cells with damaged DNA from undergoing mitosis).

All experiments were performed in triplicate, with similar results. SH-SY5Y cells were cultured in 96-well plates (5x10^5 cells/well) and incubated for 24 h in complete culture medium. After cell adhesion, LDN-87357 (0.75, 3, 6, 12, 25, 50 and 100 μM) was added to each well for 24 h; some wells received only the solvent, 0.1% DMSO (MilliporeSigma). One group of cells were exposed to 1 μM nocodazole (cat. no. M1404; MilliporeSigma) for 16 h as a positive control, and another group were cultured in complete culture medium for 24 h at 37˚C as a negative control. To evaluate the influence of the inhibitor LDN-87357 on SH-SY5Y cells in ER stress conditions, cells were transferred to 6-well plates (5x10^5 cells/well) and the culture was maintained in complete culture medium for 24 h at 37˚C.

The cultures were then pretreated with complete culture medium including LDN-87357 inhibitor at the aforementioned concentrations for 1 h at 37˚C, and then treated with 500 nM Th for 24 h at 37˚C. An additional set of cells were incubated only with 500 nM Th for 24 h at 37˚C. The SH-SY5Y cells treated with 1 μM nocodazole for 16 h at 37˚C were used as a positive control, and cells incubated for 24 h at 37˚C with complete culture were used as a negative control.

SH-SY5Y cells were then collected and rinsed twice with cold 1X DPBS (MilliporeSigma). Aliquots of 1x10^6 cells/ml were then placed in ice-cold 70% ethanol for 20 min at -20˚C. The ethanol-suspended cells were then centrifuged for 5 min at 3,630 x g at 4˚C. The remaining cell pellets were then resuspended in 250 μl of 1X DPBS, and treated with 10 mg/ml RNase A solution (cat. no. EZ0002; Canvax Reagents S.L.) and incubated for 1 h at 37˚C before they were stained using 10 μg/ml PI solution (MilliporeSigma) at 4˚C for 30 min. Finally, the samples were assessed using a CytoFLEX flow cytometer (Beckman Coulter, Inc.). The percentage of cells in each cell cycle phase (sub G0/G1, G0/G1, S and G2/M), was determined depending on the DNA content, using Kaluza Analysis Software (version 1.5A, Beckman Coulter, Inc.) and analyzed using Cyflogic™ software (version 1.2.1; CyFlo Ltd.).

Statistical analysis. All obtained results were subjected to statistical analysis using SigmaPlot (version 11.0; Systat Software, Inc.). In all the experiments performed in the present study, the normality of data distribution was determined using the Shapiro-Wilk test. As all the data were characterized by a normal distribution, further statistical analysis and comparison among multiple groups was performed using ANOVA with Dunnett's post hoc test. Correlations among changes in ER stress markers, cell survival and cell cycle data were analyzed using Pearson's correlation coefficients. Three independent tests were performed for the statistical analyses in all individual experiments. $P<0.05$ was considered to indicate a statistically significant difference among the groups.

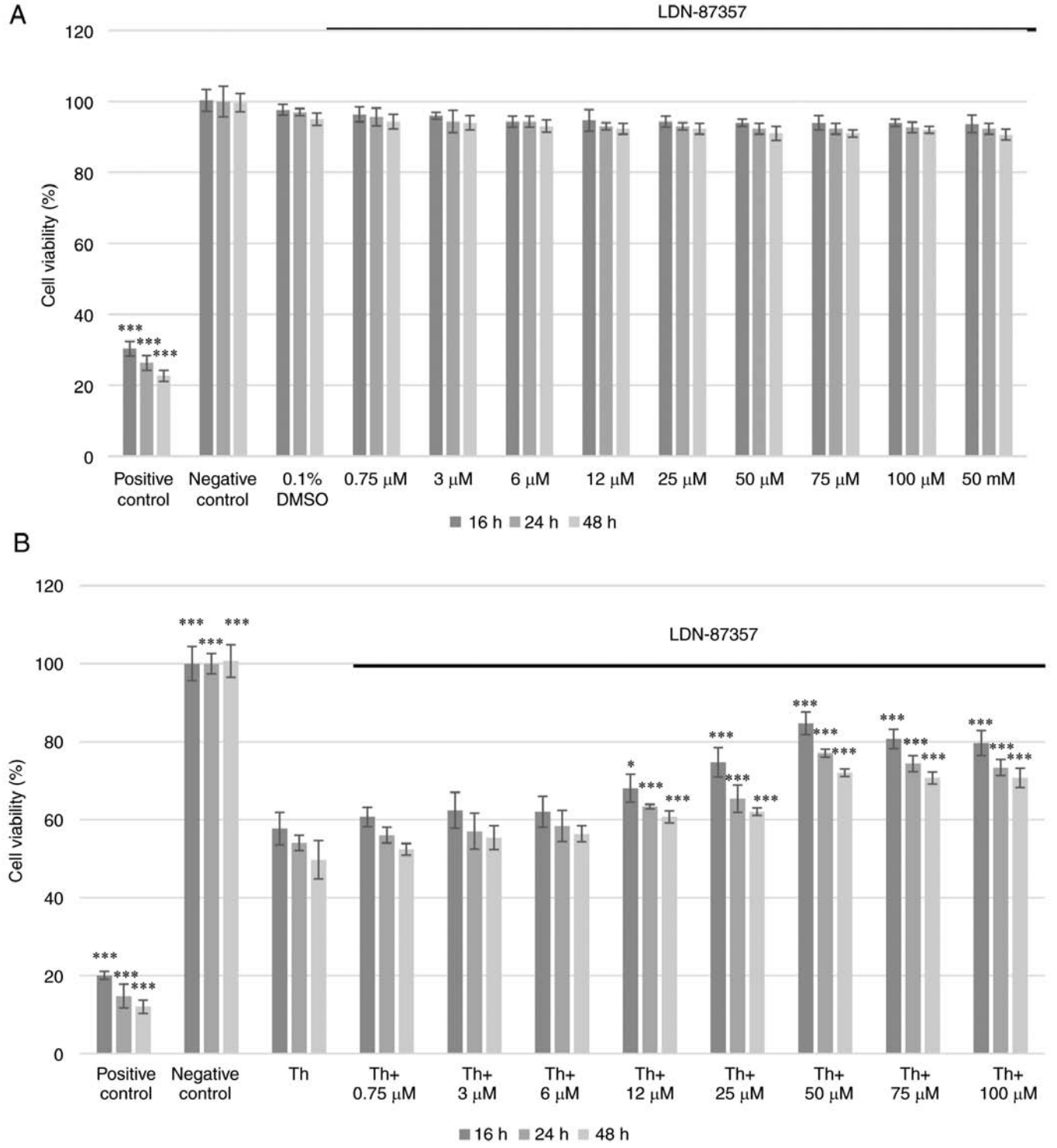

Figure 1. Analysis of the cellular toxicity of the small-molecule PERK inhibitor LDN-87357 in SH-SY5Y cells. Viability of cells treated with (A) LDN-87357 only or (B) both Th and LDN-87357 assessed using the colorimetric XTT assay. Three independent tests were performed for each statistical analysis in all the experiments. The data are presented as mean ± SE. *P<0.05, and ***P<0.001 vs. (A) negative control and (B) Th. DMSO, dimethyl sulfoxide; Th, thapsigargin.

Results

Evaluation of the cytotoxic and pharmacological effect of the inhibitor LDN-87357. The cytotoxic effect of LDN-87357 on SH-SY5Y cells was assessed using the XTT assay. No significant toxicity was demonstrated at any of the applied concentrations after 16, 24 or 48 h. Moreover, the solvent (0.1% DMSO), did not induce significant cytotoxicity either (Fig. 1A). The effect of LDN-87357 (0.75-100 μM), on cell viability was also assessed under ER stress conditions induced by Th. A significant decrease in the percentage of viable SH-SY5Y cells was demonstrated after 16, 24 and 48 h treatment with Th, compared with negative controls. However, treatment with LDN-87357 (≥50 μM) resulted in a significant increase in cell viability compared with Th treatment alone, for all incubation times (Fig. 1B).

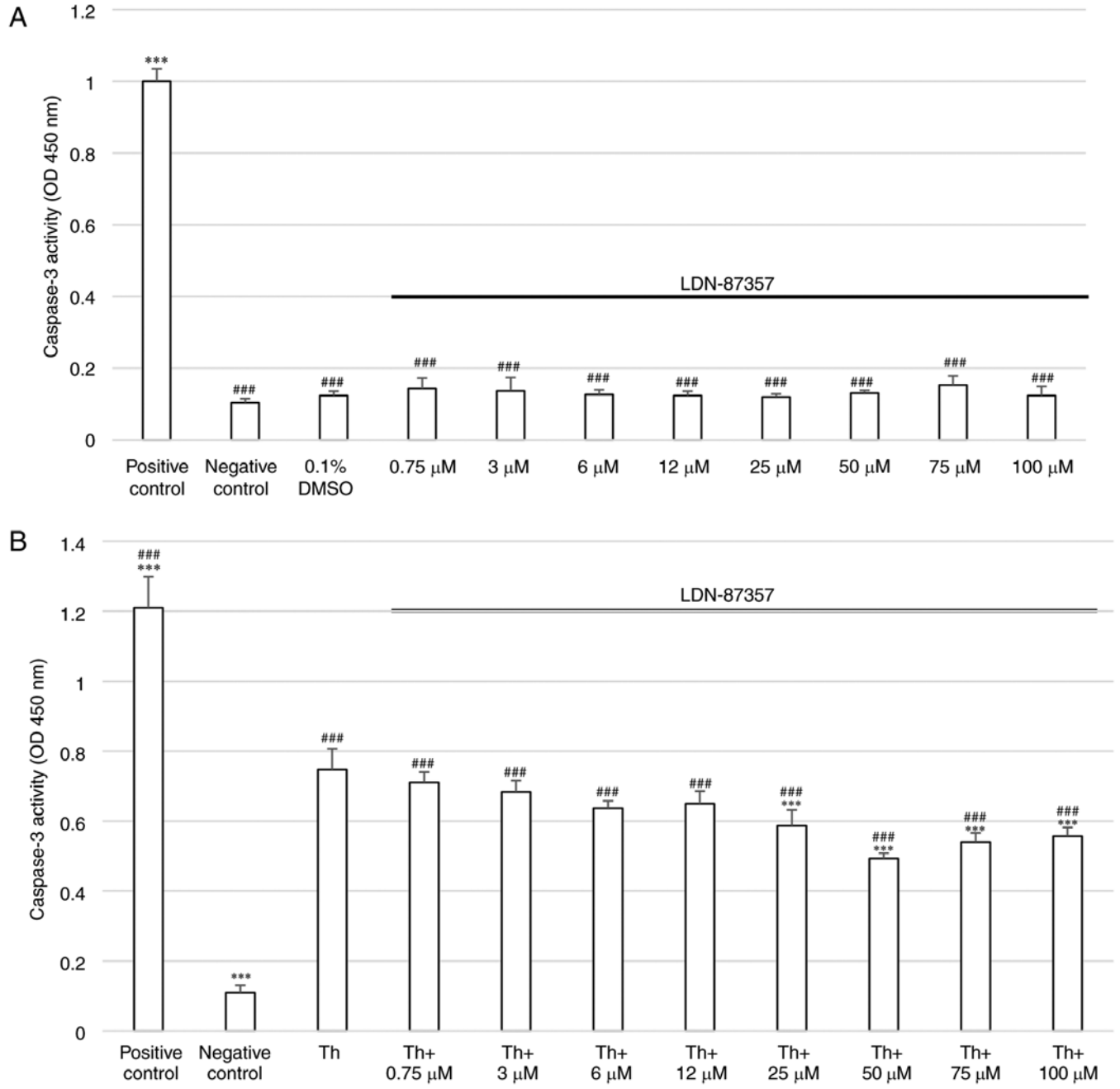

Figure 2. Analysis of apoptosis induction using the caspase-3 activity assay in the SH-SY5Y cell line. Caspase-3 activity after treatment of cells with (A) LDN-87357 alone or with (B) Th and LDN-87357. Three independent tests were performed for each statistical analysis in each of the experiments. The data are presented as mean ± SE. (A) $^{###}$P<0.001 vs. positive control, ***P<0.001 vs. negative control; (B) ***P<0.001 vs. Th, $^{###}$P<0.001 vs. negative control. The OD values were normalized to that of the positive control in (A). Th, thapsigargin; OD, optical density.

Assessment of the level of apoptosis in SH-SY5Y cells by the colorimetric caspase-3 assay. To evaluate the caspase-3 activity in SH-SY5Y cells after treatment with LDN-87357, a colorimetric caspase-3 assay was performed. The results demonstrated that SH-SY5Y cells incubated with 1 μM staurosporine for 16 h were characterized by a significant increase in the level of caspase-3 activity compared with the negative control. No significant elevation of caspase-3 activity compared with the control was demonstrated in cell cultures incubated for 24 h with LDN-87357 at any concentration. Moreover, 24 h incubation with 0.1% DMSO (the solvent used for LDN-87357) did not significantly induce caspase-3-mediated apoptosis (Fig. 2A).

Cells pretreated with Th for 16 h and then exposed to LDN-87357 (0,75-100 μM) demonstrated a significant increase in caspase 3-activity compared with the negative control cells, which were incubated with the dedicated culture medium for 24 h. However, a significant decline in caspase-3 activity was demonstrated in cells treated for 25 h with ≥25 μM LDN-87357 and Th, compared with cells treated with Th alone (Fig. 2B).

Evaluation of the effect of LDN-87357 on cell cycle distribution and progression. Treatment with LDN-87357 did not significantly affect the course of cell cycle distribution in SH-SY5Y cells. G2/M phase cell cycle arrest was only

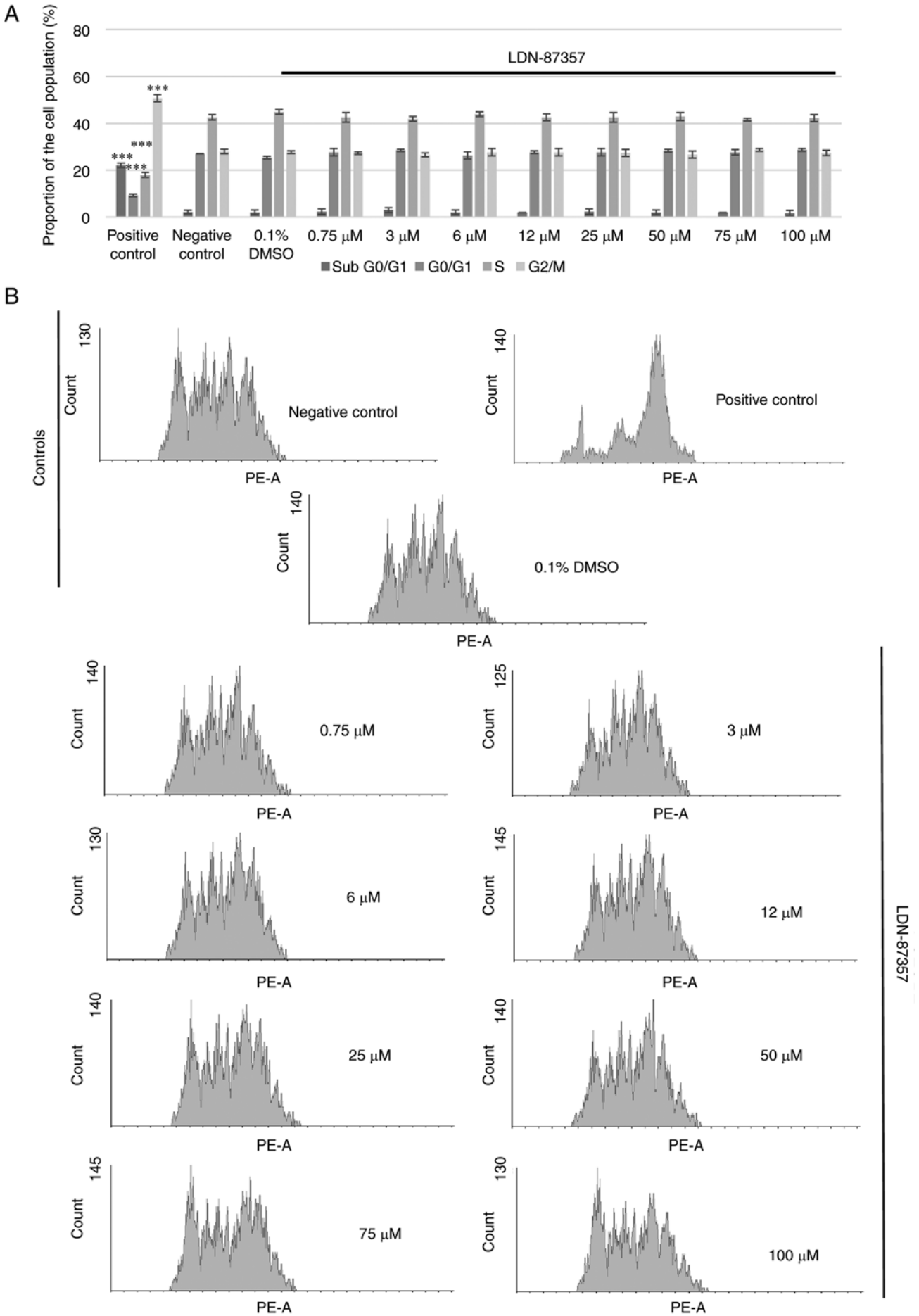

Figure 3. Continued.

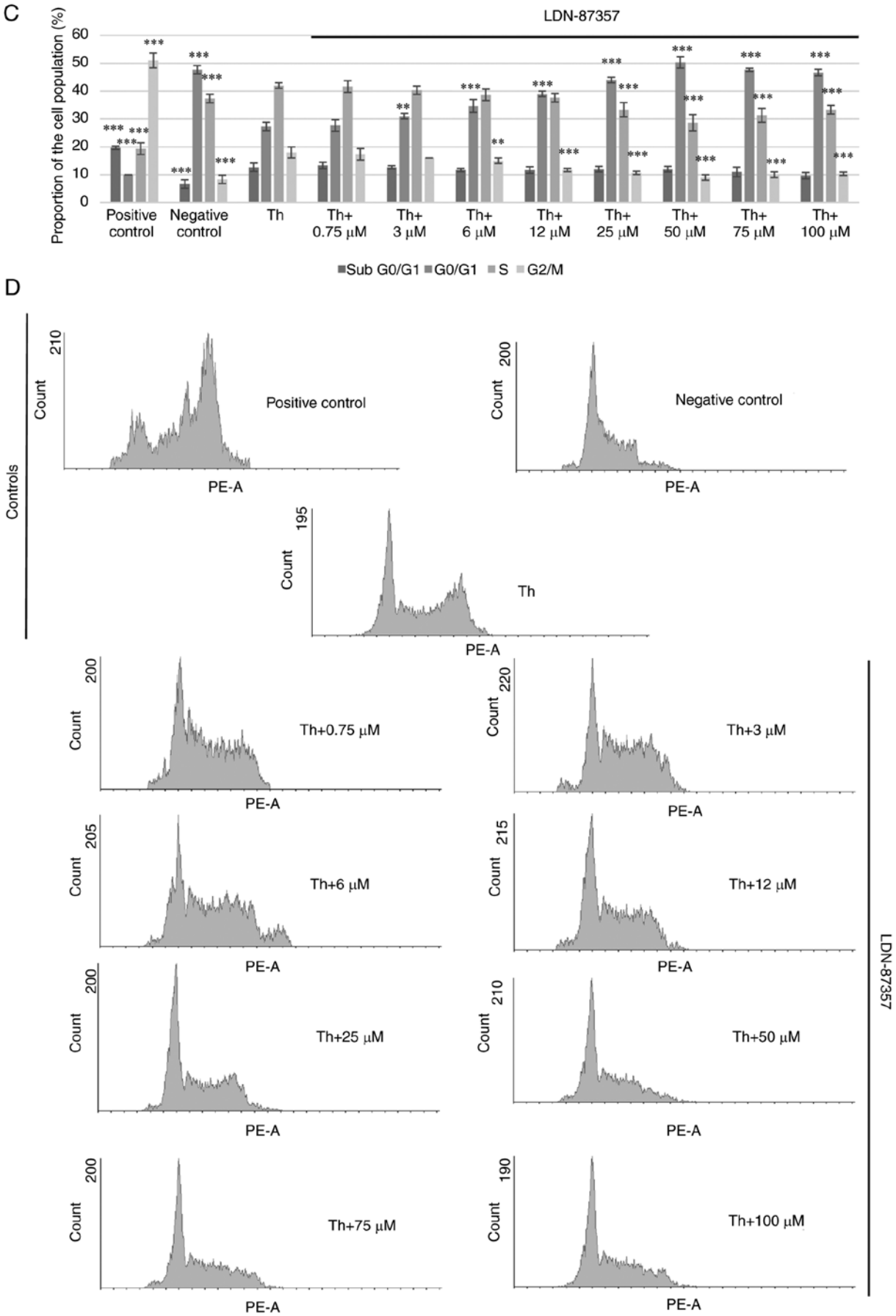

Figure 3. Flow cytometric evaluation of cell cycle distribution in SH-SY5Y cells (A) Cell cycle distribution and (B) representative flow cytometry histograms of cells treated with LDN-87357 alone. (C) Cell cycle distribution and (D) representative flow cytometry histograms of cells treated with LDN-87357 and Th. Three independent tests were performed for each statistical analysis in all experiments. The data are presented as mean ± SE. **P<0.01 and ***P<0.001 vs. (A) negative control and (B) Th. DMSO, dimethyl sulfoxide; Th, thapsigargin.

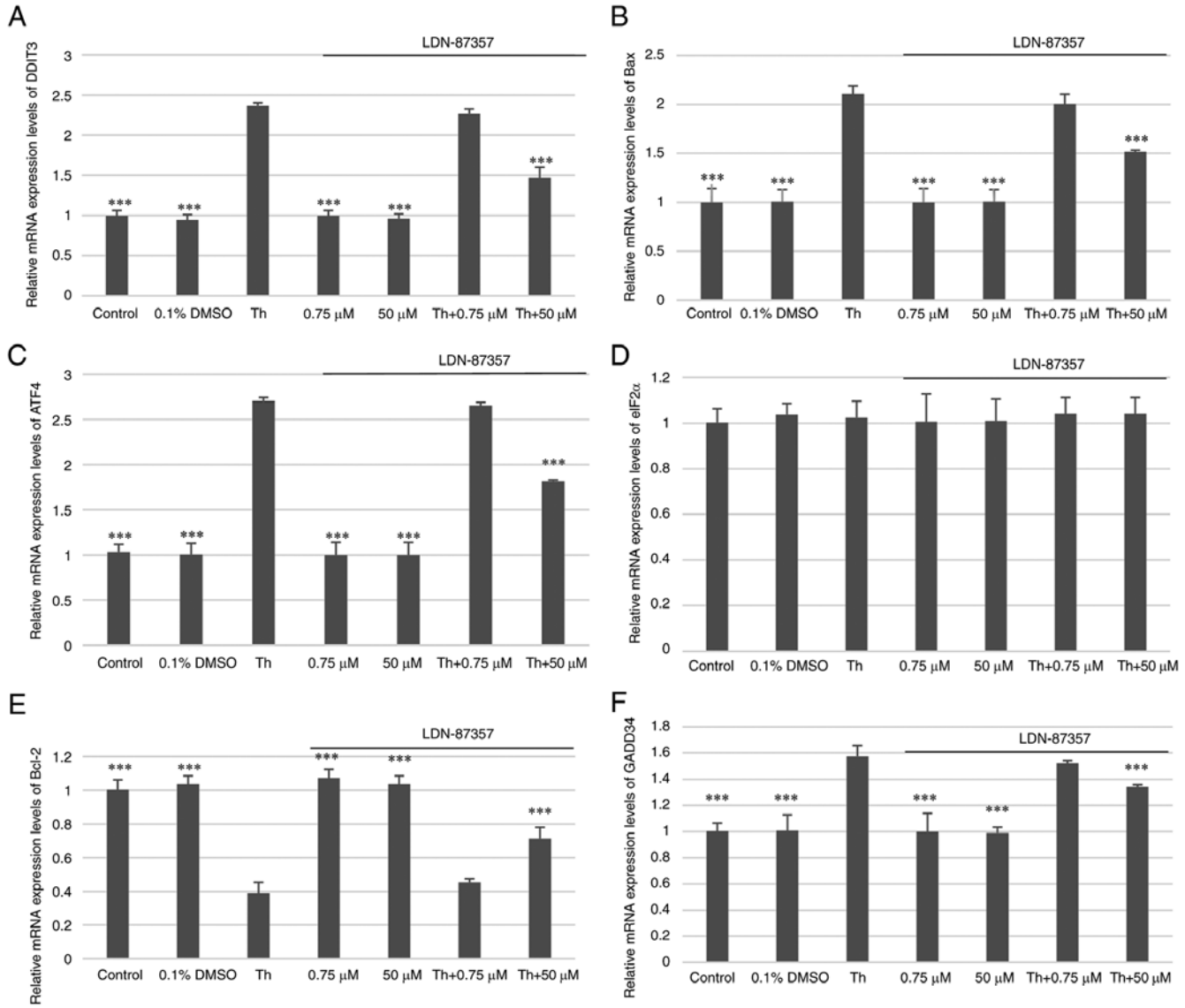

Figure 4. Analysis of the mRNA expression levels of pro-apoptotic ER stress-related genes. The relative mRNA expression levels of (A) *DDIT3,* (B) *Bax*, (C) *ATF4*, (D) *eIF2α*, (E) *Bcl-2* and (F) *GADD34* in SH-SY5Y cells with Th-induced ER stress conditions, after treatment with the small-molecule PERK inhibitor LDN-87357 alone or with both LDN-87357 and Th. The analysis was performed using the TaqMan gene expression assay. Three independent tests were performed for each statistical analysis in all experiments. The data are presented as mean ± SE. ***P<0.001 vs. Th. Untreated SH-SY5Y cells were used as the control. DMSO, dimethyl sulfoxide; Th, thapsigargin; *DDIT3, DNA damage-inducible transcript 3*; *ATF4*, *activating transcription factor 4*; *GADD34*, *DNA damage-inducible 34*.

demonstrated in the positive control sample, where SH-SY5Y cells were exposed to 1 μM nocodazole for 16 h. No significant differences in the proportion of control (cultured in complete medium) and experimental SH-SY5Y cells, exposed to LDN-87357 for 24 h were demonstrated and in each case, no cell cycle arrest was observed. Furthermore, the inhibitor solvent (0.1% DMSO) demonstrated no effect on the cell cycle course in SH-SY5Y cells after 24 h (Fig. 3A and B).

Significant cell cycle arrest at G2/M phase was demonstrated in the SH-SY5Y cells treated with nocodazole for 16 h (positive control) in comparison with the cells untreated with any compound (negative control). Furthermore, a significantly higher proportion of SH-SY5Y cells treated only with Th were found in the G2/M phase compared with the negative control. However, SH-SY5Y cells treated with Th and then with LDN-87357 (≥6 μM) for 24 h demonstrated a significant reduction in the proportion at G2/M and a significant increase in the proportion in G0/1, compared with samples incubated with Th alone (Fig. 3C and D).

The effect of LDN-87357 on the mRNA expression level of pro-apoptotic ER stress-related genes. The mRNA expression levels of *DDIT3* (encoding CHOP), *BAX, ATF4, eIF2α, Bcl-2, GADD34* in SH-SY5Y cells was quantified under Th-induced ER stress conditions, after the treatment of SH-SY5Y cells with the small-molecule PERK inhibitor LDN-87357 alone as well as after treatment with both Th and 0.75 or 50 μM LDN-87357. The pro-apoptotic genes, *DDIT3*, *Bax*, *ATF4* and *GADD34*, demonstrated a significant decrease in their mRNA expression level when treated with Th and 50 μM LDN-87357 when compared with SH-SY5Y cells treated with Th alone. However, a significant increase in the mRNA expression levels

Table II. Pearson's correlation coefficients between cell viability, cell cycle arrest and gene expression.

Parameter	Cell viability	DDIT3 expression	BAX expression	ATF4 expression	*eIF2α* expression	*Bcl-2* expression	*GADD34* expression	Population of cells in G_2/M phase
Cell viability		-1[a]	-0.999[a]	-0.998[a]	0.592	0.997[a]	-0.995	-0.999[a]
DDIT3 expression			0.999[a]	0.999[a]	-0.588	-0.997	0.995	0.999[a]
BAX expression				0.994	-0.631	-1[a]	0.999[a]	0.996
ATF4 expression					-0.546	-0.991	0.988	1[a]
eIF2α expression						0.651	-0.668	-0.556
Bcl-2 expression							-1[a]	-0.993
GADD34 expression								0.99

[a]P<0.05. Data are presented as r-values. *DDIT3*, DNA damage-inducible transcript 3; *ATF4*, activating transcription factor 4; *GADD34*, DNA damage-inducible 34.

of anti-apoptotic gene *Bcl-2* were demonstrated compared with SH-SY5Y cells treated only with Th (Fig. 4).

Pearson's correlation coefficient. The correlation between cell viability, cell cycle arrest in the G_2/M phase, and the expression levels of the pro-apoptotic (*DDIT3*, *BAX*, *ATF4*, *eIF2α*, *GADD34*) and anti-apoptotic (*Bcl-2*) genes in SH-SY5Y cells were evaluated using Pearson's correlation coefficient. Cell viability was negatively correlated with the expression levels of *DDIT3*, *BAX* and *ATF4*, and positively correlated with *Bcl-2* gene expression. Moreover, a positive correlation was detected between cell cycle arrest in the G_2/M phase and the expression levels of *DDIT3* and *ATF4*. Furthermore, cell viability and cell cycle arrest in the G_2/M phase were negatively correlated. Notably, a positive correlation was observed between the expression levels of the following genes: *DDIT3* and *ATF4*, *BAX* and *DDIT3*, *BAX* and *GADD34*. By contrast, the gene expression levels of *Bcl-2* and *ATF4*, *Bcl-2* and *GADD34* were negatively correlated (Table II).

Discussion

The present study evaluated the efficacy of the investigated small-molecule PERK inhibitor LDN-87357 in an experimental PD *in vitro* model using the human neuroblastoma SH-SY5Y cell line. The SH-SY5Y neuroblastoma cell line was used as it is one of the most commonly used *in vitro* models in PD research. SH-SY5Y is a subclone of the SK-N-SH line and it exhibits numerous characteristics of dopaminergic neurons, such as tyrosine hydroxylase and dopamine transporter expression (41,43). Other types of cells that can be used as *in vitro* models of PD include, the human HEK293, H4 and LUHMES cell lines, and rat (PC12, N27 and CSM14.1) and mouse (MN9D, Cath.a and CAD) derived cell lines (44-46). Primary dopaminergic neurons isolated from brain specimens or neurons derived from induced pluripotent stem cells (iPSCs) may also be utilized to mimic PD pathology *in vitro* (44,45). In contrast to the other aforementioned cellular models, SH-SY5Y is human-derived, dopaminergic, easily available and relatively easy to maintain in an *in vitro* culture system (41,43). The aforementioned features led to the selection of this cell line for the experiments performed in the present study.

We have previously demonstrated that treatment of SH-SY5Y cells with 500 nM Th for 2 h evoked ER stress conditions, using western blotting, which demonstrated that the protein expression level of p-eIF2α was significantly elevated compared with SH-SY5Y control cells not treated with any of the compounds (47). In the present study, the response of SH-SY5Y cells ER stress conditions induced by Th, a specific ER stress activator, was demonstrated. Th is a non-competitive inhibitor of sarco/ER Ca^{2+}-ATPase, that induces transient increases of intracellular free calcium levels; such alterations in Ca^{2+} levels serve an important role in PD pathogenesis (48,49). Treatment of SH-SY5Y cells with Th results in the induction of ER stress conditions (with elevated levels of ER stress markers, such as BiP, p-PERK/p-eIF2α, ATF4, CHOP, IRE1α/XBP1s and ATF6) and mitochondrial dysfunction, both of which have been implicated in PD pathology (50-54). It has been reported that continued exposure of dopaminergic cells to Th ultimately leads to apoptotic cell death and neurodegeneration (55). Interestingly, Th was previously reported to increase the number of αS oligomers and induce αS aggregation, which is a characteristic feature of PD (56,57).

In the present study, LDN-87357 was demonstrated to be effective in the PD model used, at the cellular level: treatment with LDN-87357 in Th-induced ER stress conditions resulted in a significant decrease in the mRNA expression levels of pro-apoptotic ER stress marker genes, including *DDIT3*, *Bax, ATF4* and *GADD34*, and a significant increase in the mRNA expression level of the anti-apoptotic *Bcl-2* gene. Furthermore, the XTT assay did not demonstrate any cytotoxic effect in SH-SY5Y cells at any concentration of LDN-87357, at any incubation period. Moreover, the colorimetric caspase-3 assay in LDN-87357 treated cells did not demonstrate any significant increase in apoptotic cell death, and treatment with Th and LDN-87357 resulted in a significant decline in the apoptotic rate, compared with treatment with Th alone.

PI staining demonstrated that LDN-87357 treatment had no significant effect on the cell cycle distribution of SH-SY5Y cells. Under ER stress conditions induced by Th, LDN-87357 treatment resulted in a significant decrease in the proportion of

cells at G2/M phase, with a simultaneous increase in the G0/1 phase, compared with cells treated with Th only. Furthermore, cell viability was negatively correlated with *DDIT3*, *BAX*, *ATF4* gene expression and positively correlated with *Bcl-2* gene expression. Moreover, there was also a positive correlation between the arrest of the cell cycle in the G2/M phase and the expression of *DDIT3* and *BAX* genes.

Therefore, it appears that LDN-87357 may significantly contribute to the limitation of the negative consequences of ER stress conditions, particularly those associated with cell apoptosis, which is a major factor in PD pathogenesis and progression (22).

Previous studies have also reported the properties of another, related small-molecule PERK inhibitor LDN-0060609 in numerous cellular models of neurodegenerative diseases. In one study, LDN-0060609 caused significant inhibition of eIF2α phosphorylation in an Alzheimer's disease (AD) model based on phenotype 1 rat normal astrocytes from diencephalon (DI TNC1) under Th-induced ER stress. Moreover, LDN-0060609 did not induce any significant increase in the apoptotic rate and had no remarkable effect on cell cycle distribution in the DI TNC1 cell line, nor did it demonstrate any toxic effect on cell viability (58). Another study examined the activity of LDN-0060609 in a mouse neuron CATH.a cell line used as an *in vitro* AD model, under ER stress conditions. The compound significantly reduced apoptosis by decreasing the protein expression level of CHOP without any cytotoxic effect (47).

LDN-0060609 was also reported to trigger marked inhibition of p-eIF2α expression in human trabecular meshwork (HTM) cells, an *in vitro* model for primary open angle glaucoma, treated with Th. Furthermore, no cytotoxic or genotoxic outcomes were reported in HTM cells at any concentration or incubation period. Moreover, the pharmacological effectiveness was confirmed by significant reversal of the negative effects of ER stress conditions induced by Th, demonstrated by increased HTM cell viability and reduced DNA damage. LDN-0060609 was also reported to restore normal cell morphology and increase proliferation in a Th-treated HTM cell line (59). Furthermore, LDN-0060609 was also reported to have caused a remarkable inhibition of p-eIF2α expression in SH-SY5Y cells, without triggering any toxic effect (47). These findings indicated the value of small-molecule PERK inhibitors as novel treatment options for neurodegenerative diseases. Extended research at the cellular level on the properties of new PERK inhibitors, such as LDN-87357, particularly regarding PD and other globally-important neurodegenerative diseases, may lead to the development of novel therapeutic approaches. The results of the present study are promising and may contribute to the growing body of knowledge regarding the use of PERK in this field. Novel neuroprotective compounds such as the small-molecule PERK inhibitor LDN-87357, which can selectively target pro-apoptotic molecules and pathways require further study.

Protein misfolding and aggregation is a key molecular mechanism widely-known to underlie the neurodegeneration process. As neurons are sensitive to protein misfolding, the resulting ER dysfunctions, ER stress and UPR activation serve a crucial role in the molecular pathogenesis of neurodegenerative diseases (21). An *in vivo* study in an A53T (missense *SNCA* gene mutation) transgenic mouse model demonstrated co-occurring αS pathology and UPR induction, supported *inter alia* by increased accumulation of polyubiquitin chains associated with ER stress (60). In a previous study which used differentiated rat sympathetic-like neuron cells (PC12), A53 αS overexpression was primarily associated with increased ROS production and impaired proteasome function; consequent ER stress induction was detected by the up-regulation of the eIF2α and ER stress-related genes*: glycine rich protein 17* and *DNA damage-inducible gene 153* (61).

The PERK-mediated branch of the UPR pathway is known to be associated with several neurodegenerative entities, such as PD (24,25,32), Alzheimer's disease (21,62) and prion disease (21,63). Numerous post-mortem studies of PD patients have confirmed that the protein expression levels of ER stress markers, especially of the PERK-dependent branch of UPR, are elevated in PD brain tissue samples (64). For instance, Hoozemans *et al* (33) reported greater immunoreactivity to the p-PERK and p-eIF2α in neuromelanin-containing dopaminergic neurons from the *SNpc* region, compared with controls. Moreover, in dopaminergic neurons, the immunoreactivities of the p-PERK and αS were colocalized.

Baek *et al* (65) reported a significant increase in the mRNA expression level of *GRP78* in the prefrontal and parietal cortex, caudate nucleus and cingulate gyrus of PD brains, which was in contrast with the GRP78 protein expression level, which was significantly decreased. These findings indicated that regulation of GRP78, a crucial chaperone for the maintenance of proteostasis, was impaired in the course of PD (65). Moreover, further post-mortem research strongly supported the role of PERK-mediated pathway in PD pathogenesis and reported that *CHOP* mRNA and protein expression levels were upregulated in the *SNpc* region (66).

However, several studies have reported interactions between αS and various UPR-related proteins. Direct interactions between αS aggregates and GRP78, associated with UPR activation, have been reported in both *in vitro* and *in vivo* models (17,35). Furthermore, downregulation of GRP78 was reported to result in a decline in exogenous αS activity, which suggested this specific ER chaperone may be a primary target of αS. Activation of the signaling cascade by GRP78 affected the morphology and dynamics of the neuronal cytoskeleton, and led to deficits in synaptic function; events which directly precede the neurodegeneration process (67).

Credle *et al* (68) reported that αS overload impaired the function of the cytoprotective factor, ATF6, which is an ER transmembrane protein and one of the three components of the UPR. ATF6 activation requires its transfer to coat protein complex II (COPII). It has been reported that αS inhibits ER stress-mediated ATF6 processing via COPII-mediated ER-Golgi transit. As a result, the pro-apoptotic signaling intensifies, while ER-associated degradation activity declines. ER-Golgi trafficking could be damaged by direct interactions between the important vesicular transit regulator ras associated binding 1 (RAB1) GTPase and αS. As a result of impaired protein maturation, ER stress conditions are induced. Furthermore, elevated expression of RAB1 was reported to result in the loss of dopaminergic neuronal protection in *in vivo* models of PD (69,70).

Paiva *et al* (71) reported that aggregated A30P αS (with a missense mutation in *SNCA*) may upregulate the expression of

the collagen type IV alpha 1 chain gene which encodes collagen IV, which is an important secretory cargo in the Golgi body. Consequently, altered ER/Golgi morphology and increased vulnerability to ER stress conditions in dopaminergic neurons have been reported.

Another well-established ER stress regulator associated with UPR activation is calcium homeostasis in the ER, which is also a major cofactor for chaperone function. An *in vivo* study on mice with knockout of the *CalbindinD9k* gene, which encodes a calcium binding protein, identified elevated intracellular calcium levels and αS overload, as well as ER-stress mediated apoptosis, in dopaminergic neurons (72). Furthermore, the calcium level appears to be disrupted by activation of the SERCA, ER calcium pump, due to αS aggregates. Subsequently, calcium reuptake by the mitochondria, which resulted in a significant increase in calcium level, enhanced ROS production and neural cell sensitization to apoptosis (36,73).

The chronically-activated PERK-dependent signaling pathway is regarded as a direct pharmacological target for neurodegenerative diseases, and it has been previously evaluated in numerous research models (74), including *in vivo* models, such as a mouse neurotoxin-based PD model (75), and frontotemporal dementia (76) and prion disease (63) models. The selective, first-in-class PERK inhibitor, 7-Methyl-5-(1-{[3-(trifluoromethyl)phenyl]acetyl}-2,3-dihydro-1*H*-indol-5-yl)-7*H*-pyrrolo[2,3-*d*]pyrimidin-4-amine (GSK2606414), is characterized by good BBB penetration and good bioavailability when administered orally (77). The compound has been tested in *in vivo* studies, including neurodegenerative diseases such as frontotemporal dementia (76) and prion disease (63) models with promising results. GSK2606414 has been reported to protect from further neuronal damage and reduce neurotoxic damage. Mercado *et al* (75) reported that GSK2606414 effectively inhibited the PERK-mediated pathway in a mouse neurotoxin-based PD model, after experimental induction of ER stress. The investigated compound protected dopaminergic neurons in the *SNpc* region, improved motor performance, and increased dopamine levels and the expression of synaptic proteins, such as synaptosomal-associated protein and vesicle-associated membrane protein 2. However, it should be noted that apart from its neuroprotective activity, treatment with GSK2606414, was associated with cytotoxicity and side effects, such as body weight loss, pancreatic toxicity and hyperglycemia in the tested animals (63,75).

Another UPR-targeting compound, the eIF2α phosphatase inhibitor Salubrinal, has been evaluated in experimental models of certain neurodegenerative processes such as AD (78) and traumatic brain injury (79). Salubrinal has also been evaluated in numerous PD experimental models with favorable results (60,61,80-82). Salubrinal use was reported to restore motor function in a mouse PD model with αS overexpression through increase of the level of p-eIF2α by growth arrest and GADD34 (60). It also upregulated ATF4 expression in the SH-SY5Y cell line (80).

Another study reported that the neuroprotective effect of Salubrinal may be associated with reduced IκB kinase activation, IκB degradation, and the resulting activation of nuclear factor-kappa B (NF-κB), rather than with the direct inhibition of the UPR pathway (83). These findings have been supported by a recent study, where Salubrinal diminished motor impairments and dopamine-related behavioral deficits in an intranigral lipopolysaccharide-induced hemi-PD rat model; however, the findings indicated that the beneficial effect could be related to a decrease in the expression of numerous factors, such as inducible nitric oxide synthase, cyclooxygenase-2 or NF-κB, as well as with the attenuation of neuroinflammation processes (82).

An alternative neuroprotective compound that has been evaluated in another neurodegenerative entity, prion disease, is the small-molecule integrated stress response inhibitor (ISRIB). ISRIB restored translation downstream of eIF2α in treated animals (84). Mechanistically, ISRIB partially restored global protein synthesis under ER stress conditions compared with GSK2606414, which completely restored the expression of CHOP and global protein synthesis. However, ISRIB had no toxic effect on pancreatic cells (85). These findings indicate the potential of PERK-mediated pathway inhibition as a selective target for achieving neuroprotection with minimized side effects (86).

A major limitation of the present study was the use of only one experimental model. Further research on LDN-87357 should include other cell lines, which replicate a PD pathology, such as genetic models and neurotoxin-based models with rotenone, 6-hydroxydopamine or 1-methyl-4-phenyl-1,2,3,6-tetrahydropirydine (87). Moreover, the results of the present study do not fully elucidate the mechanism of action of LDN-87357 and its exact molecular target in the PERK-dependent signaling pathway. Further investigation is required to evaluate *inter alia*, the expression of specific PERK-mediated pathway marker proteins. Lastly, *in vivo* studies involving PD animal models are needed to determine the pharmacokinetic and pharmacodynamic properties of LDN-87357.

Presently, the pathogenesis of PD and its involved molecular pathways are not fully understood, and current treatment strategies remain insufficient, as they focus only on progression of the disease. The results of the present study provide further details of the association between the ER stress-mediated activation of the PERK-dependent UPR signaling pathway and PD pathogenesis at the molecular level. Selective, small-molecule inhibitors of the UPR components, especially those targeting PERK, constitute an attractive option for the development of novel PD treatment strategies. Such inhibitors exhibit numerous neuroprotective effects such as chronic terminal ER stress prevention, apoptotic cell death reduction, neuroinflammation decrease, synaptic function restoration and neuronal plasticity stimulation. Previous studies have also reported that small-molecule inhibitors are characterized by good BBB penetration and bioavailability. Therefore, targeting the components of the UPR signaling pathway using small-molecule inhibitors, like the PERK inhibitor LDN-87357, may contribute to development of novel therapeutic strategies against PD.

Acknowledgements

Not applicable.

Funding

This research was funded by The Medical University of Lodz, Poland (grant no. 564/5-000-00/564-20-057), and The Polish National Science Centre (NCN): OPUS grant (grant no. 2016/21/B/NZ5/01411) and the PRELUDIUM BIS 3 grant (grant no. 2021/43/O/NZ5/02068).

Availability of data and materials

The datasets used and/or analyzed during the current study are available from the corresponding author on reasonable request.

Authors' contributions

IM and EK conceptualized the present study. IM and WRK were responsible for the methodology, and IM and EK were responsible for formal analysis. The investigation was performed by WL, WRK, GG and NS. IM and WL provided the resources used. WL, WRK, GG and NS wrote the original draft, and IM and EK reviewed and edited the manuscript. WRK and GG performed visualization of the data. IM and EK supervised the project and IM was responsible for project administration and funding acquisition. All authors have read and approved the final version of the manuscript. IM, WRK and GG confirm the authenticity of all the raw data.

Ethics approval and consent to participate

Not applicable.

Patient consent for publication

Not applicable.

Competing interests

The authors declare that they have no competing interests.

References

1. Balestrino R and Schapira AHV: Parkinson disease. Eur J Neurol 27: 27-42, 2020.
2. Aarsland D, Batzu L, Halliday GM, Geurtsen GJ, Ballard C, Ray Chaudhuri K and Weintraub D: Parkinson disease-associated cognitive impairment. Nat Rev Dis Primers 7: 47, 2021.
3. Twelves D, Perkins KS and Counsell C: Systematic review of incidence studies of Parkinson's disease. Mov Disord 18: 19-31, 2003.
4. Simon DK, Tanner CM and Brundin P: Parkinson disease epidemiology, pathology, genetics, and pathophysiology. Clin Geriatr Med 36: 1-12, 2020.
5. Dorsey ER, Sherer T, Okun MS and Bloem BR: The emerging evidence of the parkinson pandemic. J Parkinsons Dis 8 (Suppl 1): S3-S8, 2018.
6. Prakash KG, Bannur BM, Chavan MD, Saniya K, Sailesh KS and Rajagopalan A: Neuroanatomical changes in Parkinson's disease in relation to cognition: An update. J Adv Pharm Technol Res 7: 123-126, 2016.
7. Comi C, Magistrelli L, Oggioni GD, Carecchio M, Fleetwood T, Cantello R, Mancini F and Antonini A: Peripheral nervous system involvement in Parkinson's disease: Evidence and controversies. Parkinsonism Relat Disord 20: 1329-1334, 2014.
8. Cacabelos R: Parkinson's disease: From pathogenesis to pharmacogenomics. Int J Mol Sci 18: 551, 2017.
9. Jankovic J: Parkinson's disease: Clinical features and diagnosis. J Neurol Neurosurg Psychiatry 79: 368-376, 2008.
10. Tolosa E, Garrido A, Scholz SW and Poewe W: Challenges in the diagnosis of Parkinson's disease. Lancet Neurol 20: 385-397, 2021.
11. Aarsland D, Creese B, Politis M, Chaudhuri KR, Ffytche DH, Weintraub D and Ballard C: Cognitive decline in Parkinson disease. Nat Rev Neurol 13: 217-231, 2017.
12. Bloem BR, Okun MS and Klein C: Parkinson's disease. Lancet 397: 2284-2303, 2021.
13. Day JO and Mullin S: The genetics of Parkinson's disease and implications for clinical practice. Genes (Basel) 12: 1006, 2021.
14. Antony PM, Diederich NJ, Kruger R and Balling R: The hallmarks of Parkinson's disease. FEBS J 280: 5981-5993, 2013.
15. Belvisi D, Pellicciari R, Fabbrini G, Tinazzi M, Berardelli A and Defazio G: Modifiable risk and protective factors in disease development, progression and clinical subtypes of Parkinson's disease: What do prospective studies suggest? Neurobiol Dis 134: 104671, 2020.
16. Noyce AJ, Bestwick JP, Silveira-Moriyama L, Hawkes CH, Giovannoni G, Lees AJ and Schrag A: Meta-analysis of early nonmotor features and risk factors for Parkinson disease. Ann Neurol 72: 893-901, 2012.
17. Colla E: Linking the endoplasmic reticulum to Parkinson's disease and Alpha-Synucleinopathy. Front Neurosci 13: 560, 2019.
18. Malpartida AB, Williamson M, Narendra DP, Wade-Martins R and Ryan BJ: Mitochondrial dysfunction and mitophagy in Parkinson's disease: From mechanism to therapy. Trends Biochem Sci 46: 329-343, 2021.
19. Trist BG, Hare DJ and Double KL: Oxidative stress in the aging substantia nigra and the etiology of Parkinson's disease. Aging Cell 18: e13031, 2019.
20. Hou X, Watzlawik JO, Fiesel FC and Springer W: Autophagy in Parkinson's disease. J Mol Biol 432: 2651-2672, 2020.
21. Ghemrawi R and Khair M: Endoplasmic reticulum stress and unfolded protein response in neurodegenerative diseases. Int J Mol Sci 21: 6127, 2020.
22. Tsujii S, Ishisaka M and Hara H: Modulation of endoplasmic reticulum stress in Parkinson's disease. Eur J Pharmacol 765: 154-156, 2015.
23. Ni M and Lee AS: ER chaperones in mammalian development and human diseases. FEBS Lett 581: 3641-3651, 2007.
24. Mercado G, Castillo V, Soto P and Sidhu A: ER stress and Parkinson's disease: Pathological inputs that converge into the secretory pathway. Brain Res 1648: 626-632, 2016.
25. Martinez A, Lopez N, Gonzalez C and Hetz C: Targeting of the unfolded protein response (UPR) as therapy for Parkinson's disease. Biol Cell 111: 161-168, 2019.
26. Teske BF, Wek SA, Bunpo P, Cundiff JK, McClintick JN, Anthony TG and Wek RC: The eIF2 kinase PERK and the integrated stress response facilitate activation of ATF6 during endoplasmic reticulum stress. Mol Biol Cell 22: 4390-4405, 2011.
27. Jaud M, Philippe C, Van Den Berghe L, Ségura C, Mazzolini L, Pyronnet S, Laurell H and Touriol C: The PERK branch of the unfolded protein response promotes DLL4 expression by activating an alternative translation mechanism. Cancers (Basel) 11: 142, 2019.
28. Saito A and Imaizumi K: The broad spectrum of signaling pathways regulated by unfolded protein response in neuronal homeostasis. Neurochem Int 119: 26-34, 2018.
29. Gorbatyuk MS, Shabashvili A, Chen W, Meyers C, Sullivan LF, Salganik M, Lin JH, Lewin AS, Muzyczka N and Gorbatyuk OS: Glucose regulated protein 78 diminishes alpha-synuclein neurotoxicity in a rat model of Parkinson disease. Mol Ther 20: 1327-1337, 2012.
30. Rozpedek W, Pytel D, Mucha B, Leszczynska H, Diehl JA and Majsterek I: The role of the PERK/eIF2alpha/ATF4/CHOP signaling pathway in tumor progression during endoplasmic reticulum stress. Curr Mol Med 16: 533-544, 2016.
31. Szegezdi E, Logue SE, Gorman AM and Samali A: Mediators of endoplasmic reticulum stress-induced apoptosis. EMBO Rep 7: 880-885, 2006.
32. Rozpedek-Kaminska W, Siwecka N, Wawrzynkiewicz A, Wojtczak R, Pytel D, Diehl JA and Majsterek I: The PERK-dependent molecular mechanisms as a novel therapeutic target for neurodegenerative diseases. Int J Mol Sci 21: 2108, 2020.
33. Hoozemans JJ, van Haastert ES, Eikelenboom P, de Vos RA, Rozemuller JM and Scheper W: Activation of the unfolded protein response in Parkinson's disease. Biochem Biophys Res Commun 354: 707-711, 2007.

34. Gully JC, Sergeyev VG, Bhootada Y, Mendez-Gomez H, Meyers CA, Zolotukhin S, Gorbatyuk MS and Gorbatyuk OS: Up-regulation of activating transcription factor 4 induces severe loss of dopamine nigral neurons in a rat model of Parkinson's disease. Neurosci Lett 627: 36-41, 2016.
35. Bellucci A, Navarria L, Zaltieri M, Falarti E, Bodei S, Sigala S, Battistin L, Spillantini M, Missale C and Spano P: Induction of the unfolded protein response by α-synuclein in experimental models of Parkinson's disease. J Neurochem 116: 588-605, 2011.
36. Betzer C, Lassen LB, Olsen A, Kofoed RH, Reimer L, Gregersen E, Zheng J, Calì T, Gai WP, Chen T, *et al*: Alpha-synuclein aggregates activate calcium pump SERCA leading to calcium dysregulation. EMBO Rep 19: e44617, 2018.
37. Jankovic J and Tan EK: Parkinson's disease: Etiopathogenesis and treatment. J Neurol Neurosurg Psychiatry 91: 795-808, 2020.
38. Oertel W and Schulz JB: Current and experimental treatments of Parkinson disease: A guide for neuroscientists. J Neurochem 139 (Suppl 1): S325-S337, 2016.
39. Pytel D, Seyb K, Liu M, Ray SS, Concannon J, Huang M, Cuny GD, Diehl JA and Glicksman MA: Enzymatic characterization of ER Stress-dependent kinase, PERK, and development of a high-throughput assay for identification of PERK inhibitors. J Biomol Screen 19: 1024-1034, 2014.
40. Bandyopadhyay S, Ni J, Ruggiero A, Walshe K, Rogers MS, Chattopadhyay N, Glicksman MA and Rogers JT: A high-throughput drug screen targeted to the 5'untranslated region of Alzheimer amyloid precursor protein mRNA. J Biomol Screen 11: 469-480, 2006.
41. Xicoy H, Wieringa B and Martens GJ: The SH-SY5Y cell line in Parkinson's disease research: A systematic review. Mol Neurodegener 12: 10, 2017.
42. Livak KJ and Schmittgen TD: Analysis of relative gene expression data using real-time quantitative PCR and the 2(-Delta Delta C(T)) method. Methods 25: 402-408, 2001.
43. Xie B, Lin F, Peng L, Ullah K, Wu H, Qing H and Deng Y: Methylglyoxal increases dopamine level and leads to oxidative stress in SH-SY5Y cells. Acta Biochim Biophys Sin (Shanghai) 46: 950-956, 2014.
44. Slanzi A, Iannoto G, Rossi B, Zenaro E and Constantin G: In vitro models of neurodegenerative diseases. Front Cell Dev Biol 8: 328, 2020.
45. Falkenburger BH, Saridaki T and Dinter E: Cellular models for Parkinson's disease. J Neurochemistry 139 (Suppl 1): S121-S130, 2016.
46. Bai X and Strong R: Expression of synaptophysin protein in different dopaminergic cell lines. J Biochem Pharmacol Res 2: 185-190, 2014.
47. Rozpedek W, Pytel D, Diehl JA and Majsterek I: Niskoczasteczkowe inhibitory szlaku adaptacyjnej odpowiedzi na stres zaleznego od kinazy PERK jako nowatorska strategia terapeutyczna w leczeniu choroby Alzheimera. Pol Merkur Lekarski 46: 9-15, 2019 (In Polish).
48. Rivero-Rios P, Gomez-Suaga P, Fdez E and Hilfiker S: Upstream deregulation of calcium signaling in Parkinson's disease. Front Mol Neuroscience 7: 53, 2014.
49. Sun Y, Selvaraj S, Pandey S, Humphrey KM, Foster JD, Wu M, Watt JA, Singh BB and Ohm JE: MPP^+ decreases store-operated calcium entry and TRPC1 expression in Mesenchymal Stem Cell derived dopaminergic neurons. Sci Rep 8: 11715, 2018.
50. Brodnanova M, Hatokova Z, Evinova A, Cibulka M and Racay P: Differential impact of imipramine on thapsigargin- and tunicamycin-induced endoplasmic reticulum stress and mitochondrial dysfunction in neuroblastoma SH-SY5Y cells. Eur J Pharmacol 902: 174073, 2021.
51. Panagaki T, Michael M and Holscher C: Liraglutide restores chronic ER stress, autophagy impairments and apoptotic signalling in SH-SY5Y cells. Sci Rep 7: 16158, 2017.
52. Koo HJ, Piao Y and Pak YK: Endoplasmic reticulum stress impairs insulin signaling through mitochondrial damage in SH-SY5Y cells. Neurosignals 20: 265-280, 2012.
53. Chung H, Chung HY, Bae CW, Kim CJ and Park S: Ghrelin suppresses tunicamycin- or thapsigargin-triggered endoplasmic reticulum stress-mediated apoptosis in primary cultured rat cortical neuronal cells. Endocr J 58: 409-420, 2011.
54. Dibdiakova K, Saksonova S, Pilchova I, Klacanova K, Tatarkova Z and Racay P: Both thapsigargin- and tunicamycin-induced endoplasmic reticulum stress increases expression of Hrd1 in IRE1-dependent fashion. Neurol Res 41: 177-188, 2019.
55. Ullrich C and Humpel C: The pro-apoptotic substance thapsigargin selectively stimulates re-growth of brain capillaries. Curr Neurovasc Res 6: 171-180, 2009.
56. Goodwin J, Nath S, Engelborghs Y and Pountney DL: Raised calcium and oxidative stress cooperatively promote alpha-synuclein aggregate formation. Neurochem Int 62: 703-711, 2013.
57. Ito S, Nakaso K, Imamura K, Takeshima T and Nakashima K: Endogenous catecholamine enhances the dysfunction of unfolded protein response and alpha-synuclein oligomerization in PC12 cells overexpressing human alpha-synuclein. Neurosci Rese 66: 124-130, 2010.
58. Rozpedek W, Pytel D, Poplawski T, Walczak A, Gradzik K, Wawrzynkiewicz A, Wojtczak R, Mucha B, Diehl JA and Majsterek I: Inhibition of the PERK-dependent unfolded protein response signaling pathway involved in the pathogenesis of Alzheimer's disease. Curr Alzheimer Res 16: 209-218, 2019.
59. Rozpedek-Kaminska W, Galita G, Siwecka N, Carroll SL, Diehl JA, Kucharska E, Pytel D and Majsterek I: The potential role of small-molecule PERK inhibitor LDN-0060609 in primary open-angle glaucoma treatment. Int J Mol Sci 22: 4494, 2021.
60. Colla E, Coune P, Liu Y, Pletnikova O, Troncoso JC, Iwatsubo T, Schneider BL and Lee MK: Endoplasmic reticulum stress is important for the manifestations of alpha-synucleinopathy in vivo. J Neurosci 32: 3306-3320, 2012.
61. Smith WW, Jiang H, Pei Z, Tanaka Y, Morita H, Sawa A, Dawson VL, Dawson TM and Ross CA: Endoplasmic reticulum stress and mitochondrial cell death pathways mediate A53T mutant alpha-synuclein-induced toxicity. Hum Mol Genet 14: 3801-3811, 2005.
62. Smedley GD, Walker KE and Yuan SH: The role of PERK in understanding development of neurodegenerative diseases. Int J Mol Sci 22: 8146, 2021.
63. Moreno JA, Halliday M, Molloy C, Radford H, Verity N, Axten JM, Ortori CA, Willis AE, Fischer PM, Barrett DA and Mallucci GR: Oral treatment targeting the unfolded protein response prevents neurodegeneration and clinical disease in prion-infected mice. Sci Transl Med 5: 206ra138, 2013.
64. Costa CAD, Manaa WE, Duplan E and Checler F: The endoplasmic reticulum stress/unfolded protein response and their contributions to Parkinson's disease physiopathology. Cells 9: 2495, 2020.
65. Baek JH, Mamula D, Tingstam B, Pereira M, He Y and Svenningsson P: GRP78 level is altered in the brain, but not in plasma or cerebrospinal fluid in Parkinson's disease patients. Front Neurosci 13: 697, 2019.
66. Selvaraj S, Sun Y, Watt JA, Wang S, Lei S, Birnbaumer L and Singh BB: Neurotoxin-induced ER stress in mouse dopaminergic neurons involves downregulation of TRPC1 and inhibition of AKT/mTOR signaling. J Clin Invest 122: 1354-1367, 2012.
67. Bellani S, Mescola A, Ronzitti G, Tsushima H, Tilve S, Canale C, Valtorta F and Chieregatti E: GRP78 clustering at the cell surface of neurons transduces the action of exogenous alpha-synuclein. Cell Death Differ 21: 1971-1983, 2014.
68. Credle JJ, Forcelli PA, Delannoy M, Oaks AW, Permaul E, Berry DL, Duka V, Wills J and Sidhu A: α-Synuclein-mediated inhibition of ATF6 processing into COPII vesicles disrupts UPR signaling in Parkinson's disease. Neurobiol Dis 76: 112-125, 2015.
69. Cooper AA, Gitler AD, Cashikar A, Haynes CM, Hill KJ, Bhullar B, Liu K, Xu K, Strathearn KE, Liu F, *et al*: Alpha-synuclein blocks ER-Golgi traffic and Rab1 rescues neuron loss in Parkinson's models. Science 313: 324-328, 2006.
70. Gitler AD, Bevis BJ, Shorter J, Strathearn KE, Hamamichi S, Su LJ, Caldwell KA, Caldwell GA, Rochet JC, McCaffery JM, *et al*: The Parkinson's disease protein alpha-synuclein disrupts cellular Rab homeostasis. Proc Natl Acad Sci USA 105: 145-150, 2008.
71. Paiva I, Jain G, Lázaro DF, Jerčić KG, Hentrich T, Kerimoglu C, Pinho R, Szegő ÈM, Burkhardt S, Capece V, *et al*: Alpha-synuclein deregulates the expression of COL4A2 and impairs ER-Golgi function. Neurobiol Dis 119: 121-135, 2018.
72. Jung EM, Yoo YM, Park SY, Ahn C, Jeon BH, Hong EJ, Kim WY and Jeung EB: Calbindin-D9k is a novel risk gene for neurodegenerative disease. Cell Physiol Biochem 54: 438-456, 2020.
73. Giorgi C, Bonora M, Sorrentino G, Missiroli S, Poletti F, Suski JM, Galindo Ramirez F, Rizzuto R, Di Virgilio F, Zito E, *et al*: p53 at the endoplasmic reticulum regulates apoptosis in a Ca2+-dependent manner. Proc Natl Acad Sci USA 112: 1779-1784, 2015.
74. Kovaleva V and Saarma M: Endoplasmic reticulum stress regulators: New drug targets for Parkinson's disease. J Parkinsons Dis 11 (Suppl 2): S219-S228, 2021.

75. Mercado G, Castillo V, Soto P, López N, Axten JM, Sardi SP, Hoozemans JJM and Hetz C: Targeting PERK signaling with the small molecule GSK2606414 prevents neurodegeneration in a model of Parkinson's disease. Neurobiol Dis 112: 136-148, 2018.
76. Radford H, Moreno JA, Verity N, Halliday M and Mallucci GR: PERK inhibition prevents tau-mediated neurodegeneration in a mouse model of frontotemporal dementia. Acta Neuropathol 130: 633-642, 2015.
77. Axten JM, Medina JR, Feng Y, Shu A, Romeril SP, Grant SW, Li WH, Heerding DA, Minthorn E, Mencken T, *et al*: Discovery of 7-methyl-5-(1-{[3-(trifluoromethyl)phenyl]acetyl}-2,3-dihydro-1H-indol-5-yl)-7H-p yrrolo[2,3-d]pyrimidin-4-amine (GSK2606414), a potent and selective first-in-class inhibitor of protein kinase R (PKR)-like endoplasmic reticulum kinase (PERK). J Med Chem 55: 7193-7207, 2012.
78. O'Connor T, Sadleir KR, Maus E, Velliquette RA, Zhao J, Cole SL, Eimer WA, Hitt B, Bembinster LA, Lammich S, *et al*: Phosphorylation of the translation initiation factor eIF2alpha increases BACE1 levels and promotes amyloidogenesis. Neuron 60: 988-1009, 2008.
79. Wang ZF, Gao C, Chen W, Gao Y, Wang HC, Meng Y, Luo CL, Zhang MY, Chen G, Chen XP, *et al*: Salubrinal offers neuroprotection through suppressing endoplasmic reticulum stress, autophagy and apoptosis in a mouse traumatic brain injury model. Neurobiol Learn Mem 161: 12-25, 2019.
80. Wu L, Luo N, Zhao HR, Gao Q, Lu J, Pan Y, Shi JP, Tian YY and Zhang YD: Salubrinal protects against rotenone-induced SH-SY5Y cell death via ATF4-parkin pathway. Brain Res 1549: 52-62, 2014.
81. Gupta S, Mishra A and Singh S: Cardinal role of eukaryotic initiation factor 2 (eIF2α) in progressive dopaminergic neuronal death & DNA fragmentation: Implication of PERK:IRE1α:ATF6 axis in Parkinson's pathology. Cell Signal 81: 109922, 2021.
82. Cankara FN, Kuş MS, Günaydın C, Şafak S, Bilge SS, Ozmen O, Tural E and Kortholt A: The beneficial effect of salubrinal on neuroinflammation and neuronal loss in intranigral LPS-induced hemi-Parkinson disease model in rats. Immunopharmacol Immunotoxicol 44: 168-177, 2022.
83. Huang X, Chen Y, Zhang H, Ma Q, Zhang YW and Xu H: Salubrinal attenuates β-amyloid-induced neuronal death and microglial activation by inhibition of the NF-κB pathway. Neurobiol Aging 33: 1007.e9-e17, 2012.
84. Sidrauski C, Tsai JC, Kampmann M, Hearn BR, Vedantham P, Jaishankar P, Sokabe M, Mendez AS, Newton BW, Tang EL, *et al*: Pharmacological dimerization and activation of the exchange factor eIF2B antagonizes the integrated stress response. Elife 4: e07314, 2015.
85. Halliday M, Radford H, Sekine Y, Moreno J, Verity N, le Quesne J, Ortori CA, Barrett DA, Fromont C, Fischer PM, *et al*: Partial restoration of protein synthesis rates by the small molecule ISRIB prevents neurodegeneration without pancreatic toxicity. Cell Death Dis 6: e1672, 2015.
86. Hughes D and Mallucci GR: The unfolded protein response in neurodegenerative disorders-therapeutic modulation of the PERK pathway. FEBS J 286: 342-355, 2019.
87. Chia SJ, Tan EK and Chao YX: Historical perspective: Models of Parkinson's Disease. Int J Mol Sci 21: 2464, 2020.